Available online at www.sciencedirect.com
SCIENCE DIRECT®
Journal of Nuclear Materials 340 (2005) 25–32
journal of nuclear materials
www.elsevier.com/locate/jnucmat

Effects of heat input on the microstructure and toughness of the 8 MnMoNi 5 5 shape-welded nuclear steel

Karl Million [a,*], Ratan Datta [b], Horst Zimmermann [c]

[a] Welding Consultant, Am Grafenbusch 46, D-46047 Oberhausen, Germany
[b] Welding Consultant, Elsternstr. 26, D-46145 Oberhausen, Germany
[c] Welding Consultant, Genterstr. 111, D-46147 Oberhausen, Germany

Received 9 July 2004; accepted 15 October 2004

Abstract

A weld metal well proven in the German nuclear industry served as the basis for the certification of a shape-welded steel to be used as base material for manufacture of nuclear primary components. The outstanding properties of this steel are attributed to the extremely fine-grained and stable primary microstructure. Subsequent reheating cycles caused by neighbouring weld beads do neither lead to coarsened brittle structures in the heat-affected zone nor to increase in hardness and decrease in toughness, as is the case with wrought steel materials. One of the largest new reactor vessel design amongst today's advanced reactor projects is considered to be particularly suitable for the use of shape-welded parts in place of forgings. In addition the need for design and development of new shape-welded steel grades for other new generation reactor projects is emphasized, in which the experience gained with this research could make a contribution.

1. Introduction

The availability for deployment of the most mature Small Modular Nuclear Reactors (SMR) is scheduled for the end of this decade [1]. IRIS (International Reactor Innovative and Secure) is one of the several new plant designs of today's advanced reactor projects. It was announced to be a modular pressurized light water reactor with an integral primary system configuration [2–4]. All primary system components – pumps, steam generators, pressurizer, and control rod drive mechanism – are inside a large reactor vessel weighing about 1000 tons.

Recent studies are orientated at developing optimized SA 508 CL.3 type forged steels for nuclear reactor vessels [5–7]. Research efforts focus on microstructures of weld heat-affected zones (HAZs), and in particular on the coarse-grained region heated above 1100 °C, which is generally referred to as a local brittle zone (LBZ). Microstructures in the base metal HAZ of a 220 mm thick reactor pressure vessel (RPV) weld made by multi-pass narrow-gap submerged arc process were classified depending on various weld heat cycles [5]. Using ultrasonic resonant spectroscopy, it was shown that specimens with larger martensitic grain size have lower elastic constants than those with fine-grained bainite.

* Corresponding author. Tel.: +49 208 809013; fax: +49 208 801042.
E-mail address: dr.k.million@t-online.de (K. Million).

0022-3115/$ - see front matter © 2004 Elsevier B.V. All rights reserved.
doi:10.1016/j.jnucmat.2004.10.093

The degree of embrittlement in the LBZ varies with material chemistry and welding conditions. Under the conditions for the easy LBZ formation, this zones fatally affects toughness in the welded region, in which the most important microstructural factors affecting fracture toughness were the martensite fraction before PWHT (post weld heat treatment) and the carbide fraction after PWHT [6]. A study of four SA 508 CL.3 steels fabricated by vacuum-induction melting and heat treatment suggested that steels with higher strength and toughness could be processed by decreasing carbon and manganese contents and by increasing molybdenum content [7]. Another study stated that by reducing the precipitation of cementite through decreasing carbon content the ductile–brittle transition temperature (DBTT) could be lowered significantly [8]. Examining the effect of microstructure on the cleavage fracture strength of low carbon Mn–Ni–Mo bainitic steels, it was also shown that the cleavage fracture strength and DBTT were strongly affected by the alloy carbon content. The decrease in the alloy carbon content resulted in a decrease in the interlath cementite-crowded layers and higher cleavage fracture strength [9].

During the past 20 years significant progress has been made in understanding the solidification behaviour of welds and the evolution of microstructure [10–16]. The essential constituents of the primary microstructure in columnar austenite grains have been identified, and acicular ferrite was found to be the most important of them [10,11]. It is defined to be intragranularly nucleated bainite, the formation of which is favored by large austenite grains, inert behaviour of allotriomorphic ferrite at the austenite grain surface, and sufficiently high inclusion number density [12]. Recently systematic studies of inclusion in weld metal have begun [13] and phenomenological modelling of welding processes has provided unprecedented insight into understanding both the welding process and the welded materials [14]. The recognition and implementation of acicular ferrite in weld metals and wrought steels has led to considerable progress because this microstructure has the potential of combining high strength and high toughness [15]. The concept of intragranular ferrite nucleation by specific inclusions known from steel welds was transferred to the steel metallurgy [16], in order to improve the HAZ toughness in the grain coarsened field after high heat input simulation.

Acicular ferrite, this most desirable constituent of welds has proved its commercial importance with the 8 MnMoNi 5 5 weld metal. Vast majority of German primary components including the 670 mm thick narrow-gap weld of the hitherto largest reactor vessel was welded using this weld metal [17]. Based on this experience the 8 MnMoNi 5 5 was certified by the German Nuclear Safety Standards Commission (KTA) as world wide first shape-welded base material for product forms and components fabricated by shape-welding. The German Standard *KTA 3201.1 – Section 29, Product Forms and Components from ferritic steels fabricated by shape-welding* [18] applies to rotationally symmetric product forms or components that are fabricated by multiple layer deposition of molten-off electrode material and are subsequently not subjected to a heat treatment of a higher temperature than is permitted for stress-relief heat treatment (580–620 °C). As stipulated in this standard, the material is isotropic. Consequently, in the case of weld connections on components made of shape-welded parts no differences exist between base material, weld metal, and HAZs.

This German development was recently subject of a retrospective survey, building on work already published in the open literature [19]. As for the planned serial fabrication of the new IRIS reactor vessel the use of shape-welded parts in place of forging is considered to be a particularly suitable alternative, this paper presents the results of a research program conducted to investigate the primary microstructure and the reheating behaviour of this weld metal, submitting the distinct structural regions of the steel to a detailed and updated analysis. Used methods and experimental techniques could also be beneficial for development of new shape-welded nuclear steel grades for other new generation reactor projects.

2. Experimental procedure

2.1. Test material

Chemical composition and mechanical properties of the shape-welded nuclear steel 8 MnMoNi 5 5, in comparison with the traditional forged steel 20 MnMoNi 5 5 (corresponding to SA 508 CL.3) are listed in Tables 1 and 2.

Major differences in transformation behaviour of the two steels are pointed out by the CCT diagrams presented in Fig. 1(a) and (b). For both the same austenitisation temperature of 1350 °C and holding time of 1 second was used, simulating the super-reheated coarse-grained region, which is generally referred to the LBZ in the case of wrought steels. The chemical composition of the steels presented in the diagrams correspond respectively to the base material and weld metal used for the mentioned 670 mm narrow-gap joint as well as for many shape-welding applications [19]. The following flux–wire combination has been used for this development: welding flux SA FB 1 53 DC H5 (DIN EN 760), wire electrode S 3 NiMo 1 (DIN EN 756). Similar weld metal was also used for all investigations described below.

2.2. The single bead test

Taking into account that the KTA Standard recommends a limited range of heat input ($t_{8/5}$ = 7–25 s) for welding of shape-welded base materials, the effect of

Table 1
Chemical composition determined by product analysis of the forged steel 20 MnMoNi 5 5 and of the shape-welded steel 8 MnMoNi 5 5 according to KTA 3201.1 [18]

Steel type		Content, by mass, %													
		C	Si	Mn	P	S	Cr	Mo	Ni	Al_{total}	Cu	V	As	Sn	N
20 MnMoNi 5 5[a,b]	Min.	0.15	0.10	1.15	–	–	–	0.40	0.45	0.010	–	–	–	–	–
	Max.	0.25	0.35	1.55	0.012	0.012	0.20	0.55	0.85	0.040	0.12	0.020	0.025	0.011	0.013
8 MnMoNi 5 5[a,b]	Min.	0.05	–	1.00	–	–	–	0.45	0.80	–	–	–	–	–	
	Max.	0.10	0.30	1.50	0.012	0.010	0.10	0.60	1.10	0.040	0.10	0.015	0.025	0.011	0.020

[a] In the case of belt-line components, the phosphoros content should be max. 0.010%.
[b] When using the materials in the reactor pressure vessel, the contents of tantalum and cobalt shell each be max. 0.030%.

Table 2
Mechanical properties of the forged steel 20 MnMoNi 5 5 and of the shape-welded steel 8 MnMoNi 5 5 according to KTA 3201.1 [18]

Steel type	Temperature (°C)	0.2% – Proof stress $Rp_{0.2}$ (N/mm^2) min.		Tensile strength R_m (N/mm^2)	Elongation at fracture A5 (%) min.		Reduction of area Z (%) min.	Absorbed impact energy (J) min.	
		Max. 320	Max. 650	Max. 650	Max. 320	>320 Max. 650		Single value	Average value of three test specimens
20 MnMoNi 5 5	0	–	–	–	–	–	–	34	41
	20	390	390	560–700	19	19	45	–	–
	350	343	314	Min. 505	16	14	–	–	–
8 MnMoNi 5 5	0	–		–	–		–	100	120
	20	480		570–700	20		65	120	150
	350	390		Min. 510	17		–	–	–

three different thermal cycles on primary microstructure of single beads has been investigated: (a) $t_{8/5}$ = 15.8 s, corresponding to a heat input of 2.80 kJ mm^{-1}; (b) $t_{8/5}$ = 22.6 s, corresponding to a heat input of 4.25 kJ mm^{-1}; (c) $t_{8/5}$ = 43.6 s, corresponding to a heat input of 6.65 kJ mm^{-1} (average values of each three $t_{8/5}$ measurements). The first $t_{8/5}$ time (15.8 s) corresponds approximately to welding parameters used for production welds, both for joining welds and shape-welding applications (5 mm diameter wire electrode; 750 A current; 32 V DC; 8.7 mm s^{-1} welding speed). For the other two $t_{8/5}$ times (22.6 and 43.6 s) double and triple wire electrodes of 4 mm (parallel arrangement) and increased welding current (1150 A and 1800 A) were used, respectively, without changing the arc voltage and the weld speed. All test welds were deposited at the same preheating temperature of 100 °C and maximum interpass temperature of 250 °C.

To enable such single beads to be tested in representative conditions they were deposited on a 130 mm thick shape-welded material of equal chemical composition (described below more closely). In order to facilitate the accommodation of Charpy-V notch (CVN) specimens (10 × 10 × 55 mm^3) inside of single beads, as shown in of Fig. 2, the beads were deposited along a machined depression (interrupted line in Fig. 2). To verify in addition the effect of stress-relief annealing on microstructure and toughness, a heat treatment deliberately carried out at elevated temperature and over a longer duration (650 °C for 8 h, heating rate 50 C° per hour, furnace cooling down to 100 °C) was used. The notch-impact energy was investigated at temperatures between −30 °C and +50 °C (average of three individual results for each temperature).

2.3. Multilayer test coupon

As for future applications mainly shape-welding by axial material build-up (vertical axis of rotation) comes into consideration [19], a corresponding test coupon was fabricated and examined in detail by optical microscopy and CVN tests. Fig. 3 illustrates schematically this approach.

In order to verify at the same time the effect of heat input near to its upper limit ($t_{8/5}$ = 25 s), the test coupon was manufactured using welding parameters corresponding to a cooling time $t_{8/5}$ = 22.6 s (double wire electrodes of 4 mm, welding current 1150 A). A working temperature between 150 and 250 °C was maintained during welding. To verify again the effect of stress-relief

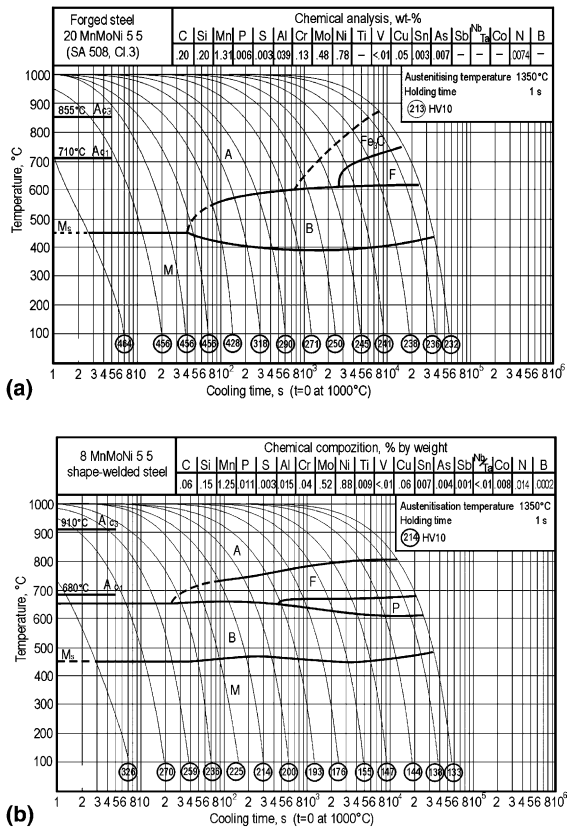

Fig. 1. CCT diagrams of the compared two steels [20].

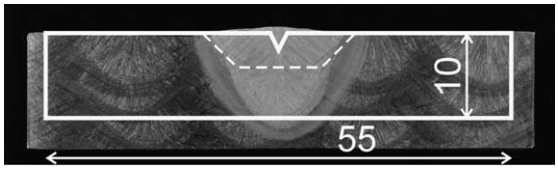

Fig. 2. Macro-section of an 8 MnMoNi 5 5 single weld bead deposited on shape-welded base metal, illustrating the location of Charpy-V specimen.

annealing on microstructure and toughness, a heat treatment at 600 °C for holding time of 3×6 h was used. This time the impact tests were made at −12 °C in order to corroborate the comparison with the required minimum values at 0 °C (Table 2).

3. Results and discussion

3.1. Primary microstructure

Comparing the chemical composition of the two steels (Table 1) it stands out that the shape-welded version is

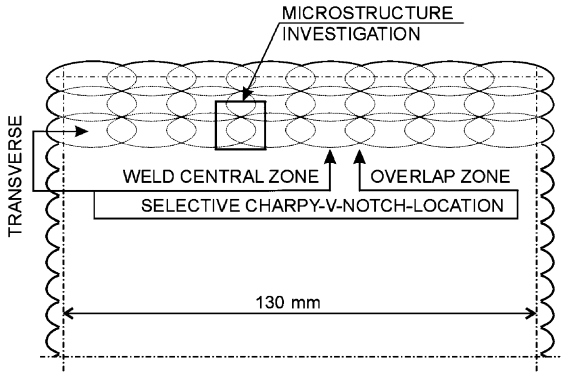

Fig. 3. Schematic diagram of the test coupon manufactured by axial material build-up and examined metallographically and by CVN tests.

characterised mainly by minimized carbon content (0.05–0.10%). Due to the well known sensitivity to carbon of low alloyed weld metal [11] the reduction of the carbon concentration improves radically the welding behaviour of the 8 MnMoNi 5 5 shape-welded steel, which is confirmed by the CCT diagrams presented in Fig. 1. While the forged steel, Fig. 1(a), achieves hardness values over 450 HV10, the shape-welded steel exhibits maximum hardness values of less than 350 HV10. This forms the basis for the exceptionally reliable crack resistance of the 8 MnMoNi 5 5 without any risk of LBZ occurrence, and for its considerably enhanced toughness reserves in comparison with the forged steel (Table 2).

The primary microstructure of single beads generated by welding with normal and with excessive heat input is exemplified in Fig. 4. In both cases ($t_{8/5} = 15.8$ s and $t_{8/5} = 43.6$ s) typical large columnar grains are identifiable as well as thin allotriomorphic ferrite layers at the grain boundaries. The increase of heat input causes a visible rise in thicknesses of grain boundary ferrite layers, without affecting significantly either the size of austenitic grains nor the microstructure within the grains. At increased magnification, as shown in Fig. 5, a detail of the allotriomorphic ferrite at the grain boundary, as well as the very fine-grained acicular ferrite in the grain interior are identifiable. Widmanstätten ferrite was not found in the as-deposited conditions, or does occur in negligible and not easy identifiable amount, being probably widely suppressed by the intragranular bainite formation. The formation of this type of primary microstructure was already studied in detail several years ago [12], establishing that its formation is promoted by three main factors: the relatively large size of the austenite grains, the presence of a relatively high inclusion density (serving the heterogeneous intragranular nucleation of acicular ferrite), and the presence of a layer of inert allotriomorphic ferrite at the austenite grain surfaces (causing a transition from bainite to acic-

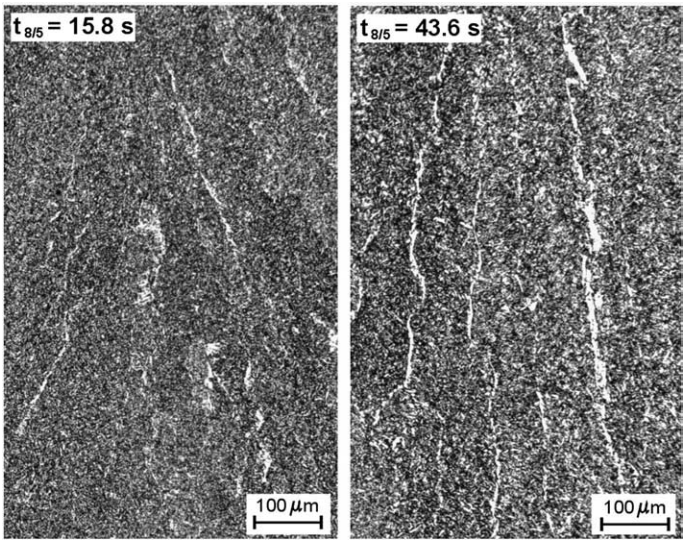

Fig. 4. Primary microstructure in the central region of single beads corresponding to usual ($t_{8/5}$ = 15.8 s) and to excessive ($t_{8/5}$ = 43.6 s) heat input.

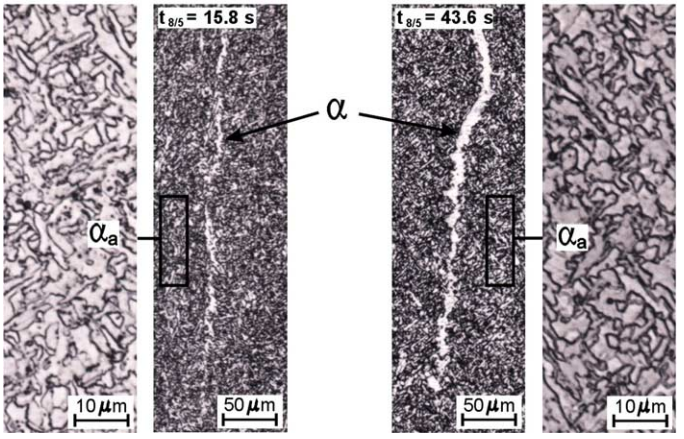

Fig. 5. Primary microstructure at columnar grain boundaries in the central region of single beads corresponding to usual ($t_{8/5}$ = 15.8 s) and to excessive ($t_{8/5}$ = 43.6 s) heat input α – allotriomorphic ferrite at grain boundaries; α_a – acicular ferrite (intragranularly nucleated bainite).

ular ferrite, i.e. bainite nucleation in the interior of the austenite grain instead of its nucleation at the grain boundary).

At higher magnification power (magnified display details in Fig. 5) it becomes apparent that in the as-deposited state the size of acicular ferrite plates is slightly increased when welding with excessive heat input ($t_{8/5}$ = 43.6 s).

Similar microstructural behaviour was found after stress-relief annealing of single beads, as shown in Fig. 6. In all micrographs the presence of oxide inclusions affirmed the importance of optimized oxygen contents [13] in the 8 MnMoNi 5 5 submerged arc-weld metal.

The effect of heat input variations is more precisely to quantify by means of single bead CVN tests. This results are summarized in Fig. 7. A single bead which is welded using standard parameters (single wire electrode) and usual heat input ($t_{8/5}$ = 15.8 s) comes to highest toughness values, both in as-deposited conditions and after PWHT.

The fact that single bead CVN values react susceptibly to heat input variations proves the severe character of the test method and its suitability to verify the toughness behaviour of shape-welded steels or the welding technology to be used for further processing of shape-welded steels. The results affirm that for a well designed

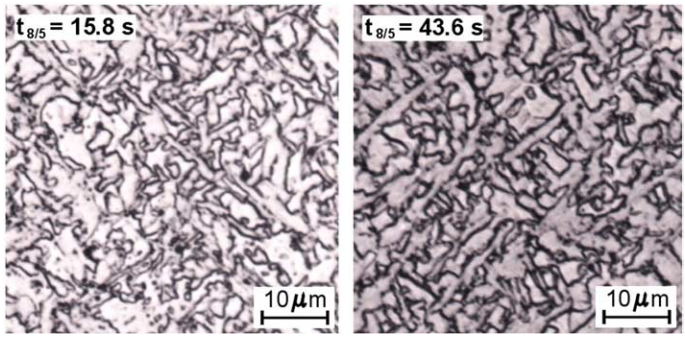

Fig. 6. Microstructure after stress-relief annealing in the central region of single beads corresponding (on the left) to usual and (on the right) to excessive heat input.

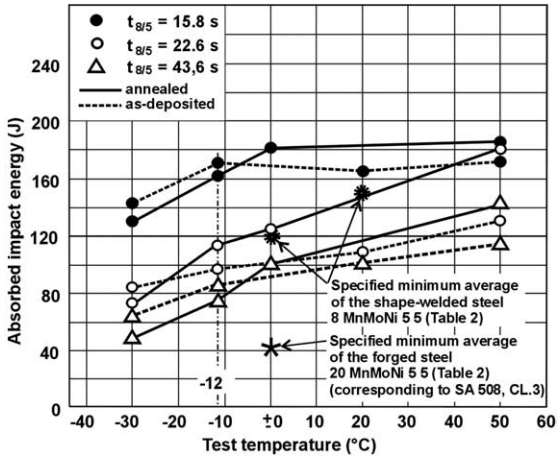

Fig. 7. Effect of heat input on Charpy toughness (CVN) of single weld beads in as-deposited and in annealed conditions.

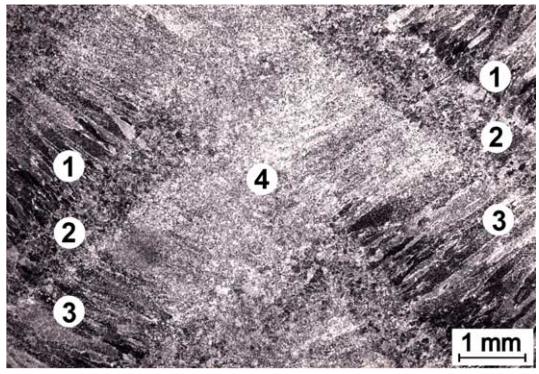

Fig. 8. Magnified detail from Fig. 3 containing all four structural regions: 1 – FZ; 2 – cgHAZ; 3 – fgHAZ; 4 – ovHAZ.

shape-welded steel it is not enough to obtain acicular ferrite in the primary microstructure, but also as thin as possible layers of inert allotriomorphic ferrite.

3.2. Reheating effects in multilayer material

Four main structural zones are distinguished on the magnified detail presented in Fig. 8: (1) – FZ (fusion zone consisting of non-transformed weld metal); (2) – cgHAZ (coarse-grained heat-affected zones, reheated far above A_{C3} up to near the melting point, characterized as LBZ in the case of wrought steels); (3) – fgHAZ (fine-grained heat-affected zones, reheated above A_{C1} into a grain-refining temperature range); (4) – ovHAZ (overlapping heat-affected zones). Especially the complex nature of the ovHAZ (4) formed by mutual overlapping of cgHAZs (2) and fgHAZs (3) is visible in this picture. It appears at the relatively low optical magnification that the columnar fusion zone (1) has the largest grain size, whereas in the neighbouring over reheated coarse-grain zone (2) smaller non-columnar austenitic grains occur. Under it, in zone (3), the columnar character of the reheated material seems to be maintained although it was reheated above A_{C1} into a grain-refining temperature range.

It is striking, that except zone (1) – FZ – the thermal history of the other three zones becomes less pronounced at higher magnifying power, as visible in the micrograph examples presented in Fig. 9. It is again affirmed in zone (1) that acicular ferrite is the dominating phase within the entire volume of columnar grains. Besides in zone (1), the allotriomorphic ferrite layer at the grain boundary appears to be inert, as no signs for intergranular nucleation of bainite or Widmanstätten ferrite have been found. Systematically less pronounced and discontinuous ferritic grain boundaries occur in all other zones (2, 3, and 4), and less acicular and more granular character of bainitic ferrite is detected inside the grains. Sporadically intergranular bainite and even isolated Widmannstätten ferrite formation were identified in zone (2). It is difficult to state more precisely the history of this transformations, because of the widely diversified possible temperatures involved. Using selec-

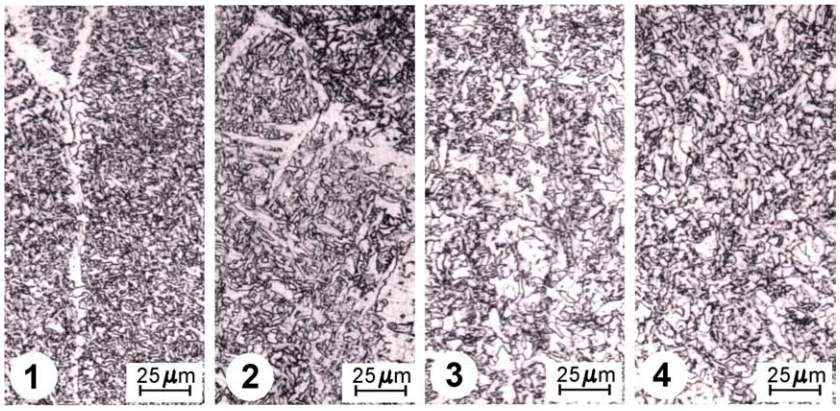

Fig. 9. Micrographs of the four structural regions from Fig. 8: 1 – FZ; 2 – cgHAZ; 3 – fgHAZ; 4 – ovHAZ.

tive heat treatments the aforementioned research work has shown [12] that allotriomorphic ferrite was activated by annealing at 760 and 750 °C, and bainite shaves have formed as a consequence. However in zone (2), the smaller size of austenite grains seems to affect the inert character of the allotriomorphic ferrite.

As well, like in the case of single bead investigations no significant microstructural changes have been found due to PWHT.

The results obtained with CVN tests using selective notch locations (according to Fig. 3) are summarized in Fig. 10. This test series affirm the results obtained with single bead CVN tests and allow following amendments:

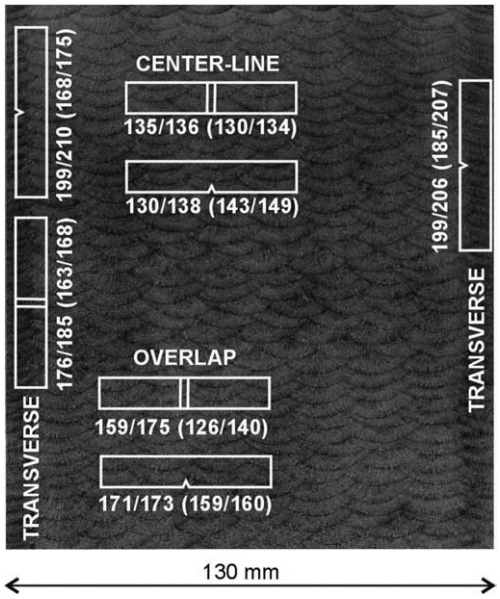

Fig. 10. Macrograph of an 8 MnMoNi 5 5 shape-welded test coupon manufactured by axial material build-up, stating the CVN values (J) at −12 °C (smallest single value/average value) after PWHT (600 °C, for 3 × 6 h); values in brackets are results obtained before PWHT.

- increased heat input even near to the permitted upper limit ($t_{8/5}$ = 25 s) does not have a significant effect neither on the microstructure nor on the toughness behaviour of the shape-welded steel 8 MnMoNi 5 5;
- unlike single beads, no CVN values below the required minimum have been detected in multilayer material confirming the beneficial effect of multilayer welding;
- transverse notch orientation to columnar grains results systematically in highest CVN values even at increased heat input, confirming the result made with single bead that the loss of toughness at increased heat input is caused by intergranular and not intragranular structural changes;
- no essential change in toughness occurred due to stress relieving, which complies with similar results obtained in C–Mn all-weld deposits when optimum carbon and manganese content was retained [21].

4. Conclusions

The results confirm that for a well designed 8 MnMoNi 5 5 shape-welded steel it is not sufficient to obtain acicular ferrite in the primary microstructure, but it is necessary to get at the same time grain boundaries with thin enough and inert layers of allotriomorphic ferrite; excessive heat input causes increased grain boundary layer thickness having detrimental effects on the toughness behaviour of the steel.

The considerably enhanced toughness reserves of the shape-welded steel represent the essential selection criterion for future applications and new developments; this superior criterion has to be fulfilled already by single beads in as-deposited conditions.

For this purpose the single bead test described in this paper offers a simple method for selection of feed materials (flux–wire combination) as well as for development and survey of manufacturing technologies.

References

[1] A Department of Energy (DOE) Report, Nuclear News 44 (9) (2001) 25. Available from: http://www.ans.org/pubs/magazines/nn/docs/2001-8-2.pdf.

[2] M.D. Carelli, Nuclear News 46 (10) (2003) 32.

[3] J.M. Collado, in: Proc. Int. Congress on Advanced Nuclear Power Plants (ICAPP03), Congress Palais, Córdoba, Spain, 4–7 May 2003, University of Florida, USA, 2003.

[4] A.C.O. Barosso, B.D. Baptista F°, I.D. Arone, L.A. Macero, P.A.B. Morares, in: Proc. Int. Congress on Advanced Nuclear Power Plants (ICAPP03), Congress Palais, Córdoba, Spain, 4–7 May 2003, University of Florida, USA, 2003.

[5] Y.-M. Cheong, J.-H. Kim, J.-H. Hong, H.-K. Jung, in: Proc. 15th World Conference on Non-destructive Testing, Roma, Italy, 15–17 October 2000, AIPnD – Italian Society for Non-Destructive Testing and Monitoring Diagnostics, Brescia, Italy, 2000.

[6] S. Kim, S.-Y. Kang, S.J. Oh, S. Lee, J.-H. Kim, J.-H. Hong, Metall. Mater. Trans. 31A (2000) 1107.

[7] S. Kim, Y.-R. Im, S. Lee, H.-C. Lee, Y.-J. Oh, J.-H. Hong, Metall. Mater. Trans. 32A (2001) 903.

[8] Y.-R. Im, Y.-J. Oh, B.-J. Lee, J.-H. Hong, H.-C. Lee, J. Nucl. Mater. 297 (2001) 138.

[9] Y.-R. Im, B.-J. Lee, Y.-J. Oh, J.-H. Hong, H.-C. Lee, J. Nucl. Mater. 324 (2004) 33.

[10] H.K.D.H. Badheshia, L.-E. Svenson, B. Gretoft, Acta Metall. 33 (1985) 1271.

[11] H.K.D.H. Badheshia, Weld. J. 83 (9) (2004) 237s.

[12] S.S. Babu, H.K.D.H. Badheshia, JIM 32 (8) (1991) 679.

[13] T. Hong, T. Debroy, S.S. Babu, S.A. David, Metall. Mater. Trans. 31B (2000) 161.

[14] S.A. David, S.S. Babu, J.M. Vitek, JOM 55 (6) (2003) 14.

[15] C.H. Lee, H.K.D.H. Badheshia, H.-C. Lee, Mater. Sci. Eng. A 360 (2003) 249.

[16] C. Van der Eijk, Ø. Grong, S.A. David, in: Proc. 5th International Conference on Trends in Welding Research, Georgia, USA, 1–5 June 1998, ASM International, Materials Park, OH 44073-0002, USA.

[17] H. Hantsch, K. Million, H. Zimmermann, Weld. J. 61 (7) (1982) 27.

[18] KTA 3201.1 (06/98): Components of the Reactor Coolant Pressure Boundary of Light Water Reactors, Part 1: Materials and Product Forms, Chapter 29 – Product forms and components from ferritic steels fabricated by shape-welding, p. 98. Safety Standards of the Nuclear Standards Commission (KTA), in: KTA-Geschäftsstelle c/o Bundesamt für Strahlenschutz (BfS) (Ed.), Salzgitter, Germany. Available from: http://www.kta-gs.de/e/standards/3200/3201_1e.pdf.

[19] R. Datta, K. Million, H. Zimmermann, Weld. Cutting 55 (4) (2003) 216.

[20] K. Million, H. Zimmermann, in: Proc. 5th Int. Conf. Welding in Nuclear Engineering, Nürnberg, 26–28 November 1986, DVS-Berichte 106 (1986), p. 92.

[21] G.M. Evans, Weld. J. 65 (1986) 326s.